Adsorption and surface alloying of lead monolayers on (111) and (110) faces of gold

1974 J. Phys. F: Met. Phys. 4 798

(http://iopscience.iop.org/0305-4608/4/5/022)

J. Phys. F: Metal Phys., Vol. 4, May 1974. Printed in Great Britain.

Adsorption and surface alloying of lead monolayers on (111) and (110) faces of gold

J Perdereau, J P Biberian† and G E Rhead

Université de Paris VI, Ecole Nationale Supérieure de Chimie, Laboratoire de Métallurgie et Physico-Chimie des Surfaces, 11, rue Pierre et Marie Curie, 75231 Paris Cedex 05, France

Received 13 July 1973, in final form 9 November 1973

Abstract. Auger electron spectroscopy and low energy electron diffraction have been used to study monolayers of lead deposited in ultrahigh vacuum on to (111) and (110) faces of gold. Comparison is made with a previous study of the (100) substrate. The succession of structures is similar on all three faces: low density arrangements followed by a compact hexagonal monolayer followed by another hexagonal arrangement which is interpreted as the intermetallic compound $AuPb_2$. (A previous interpretation in terms of $AuPb_3$, based on observations on the (100) face, is corrected). The completion of the first monolayer is marked by sharp knees in the plots of the Auger signals as a function of evaporation time. Essentially the same alloy structure is found on all three faces. There are only slight differences due to differences in the substrate symmetry and structure.

1. Introduction

In a previous paper (Biberian and Rhead 1973), to be referred to as BR) we described the first stages in the ultrahigh vacuum deposition of lead on to a (100) gold substrate and we have reported a surface alloying phenomenon that occurs after completion of the first dense monolayer. In the present study we have extended the investigation to the (111) and (110) substrates.

The experimental conditions and techniques are the same as those described by BR. The cleaned surface of a gold single crystal (cut to within 1° of a low index orientation) is exposed in an ultrahigh vacuum chamber to a beam of lead vapour from a simple evaporating source. In a typical experimental run a series of depositions is made, in steps of about 0·1 monolayer, under conditions of constant vapour flux. After each deposition the surface is examined by low energy electron diffraction (LEED) and by Auger electron spectroscopy (AES).

We recall the main experimental details: a Varian LEED chamber with the facility for AES provided by the retarding grid method (modulation 2 V RMS); the Auger spectra are obtained by using the LEED gun operated at 550 V as the source of primary excitation; the residual gas pressure is less than 10^{-9} Torr; the specimen is mounted on a precision manipulator with micrometer displacements; both the lead and the gold are 99·999% pure; the lead is evaporated from a crucible typically at 600 °C, placed at 15 cm from the

† Permanent address: Département de Physique, Centre Universitaire de Marseille, Luminy, 13009 Marseille, France.

gold crystal; the deposition can be interrupted by turning the crystal or by rotating a cover over the lead source; the depositions are made with the substrate at ambient temperature. At the end of a run the surface is cleaned by argon ion bombardment.

2. LEED patterns and their interpretation

For each of the two substrate orientations the sequence of LEED patterns was found to be readily reproduced in a series of at least ten successive runs. In one experiment, three specimens, with orientations (100), (111) and (110), were mounted side by side on the same specimen holder. (It had previously been verified by AES that the vapour flux varied by less than 10% over the area occupied by the specimens). A typical set of results obtained by simultaneously depositing on these three specimens is shown in table 1.

Table 1. LEED patterns: time (min) at which pattern is first observed

Time†	(100)	(111)	(110)
0	$p(\sim 5 \times \sim 20)$	$p(\sim 20 \times \sim 20)\ R\ 30°$	$p(1 \times 2)$
0·5		$p(1 \times 1)$	$p(1 \times 3)$
0·75	$p(1 \times 1)$	$p(\sqrt{3} \times \sqrt{3})\ R\ 30°$	
1·25	$c(2 \times 2)$		$p(1 \times 1)$
1·50	$c(7\sqrt{2} \times \sqrt{2})\ R\ 45°$	figure 1(*a*)	$p(7 \times 1)$
1·75	$c(3\sqrt{2} \times \sqrt{2})\ R\ 45°$		
2·00	$c(6 \times 6)$		$p(7 \times 3)$ (figure 1(*b*))
2·25			$p(4 \times 4)$ (figure 1(*c*))
3·00	hexagonal '12 spots'	hexagonal '6 spots'	hexagonal '12 spots' (figure 4(*b*))
4·00		hexagonal '12 spots' (figure 4(*a*))	

† As in the previous work (BR) the vapour source was not independently calibrated. The times are meaningful only on a relative scale.

The patterns first obtained after cleaning and before starting the deposition are all characteristic of anomalous structures believed to be due to a reconstruction of the top layer of the clean surface (see for example Grønlund and Nielsen 1973, Rhead 1973). The pattern observed for the cleaned (111) substrate—essentially a $p(1 \times 1)$ pattern with poorly resolved satellite spots—has not been reported previously. The pattern can be interpreted in terms of an hexagonal overlayer of gold with the crystalline parameter contracted by about 5%—this is the same interpretation that has been proposed for the anomalous (100) surface (Palmberg and Rhodin 1967, 1968).

In table 1 we have noted the times of first appearance of the various patterns. A certain overlap occurs between successive structures; they can coexist for short ranges of coverage. The nomenclature due to Wood (1964) is used to describe the patterns. The column for the (100) face reproduces the results of BR. The interpretations made for that face are easily transferred to the other low index orientations: first the 'anomalous' structure is transformed to the 'normal' structure characteristic of a bulk low index plane then, as the deposition progresses, there occur low density arrangements followed by a compact monolayer arrangement. Finally, a hexagonal pattern is obtained which is essentially

the same on each of the three faces. This is the pattern that has been interpreted, for the (100) face, as a surface alloy.

The transition from the 'anomalous' to 'normal' ie $p(1 \times 1)$, structure has been commented upon by BR. In the case of the (111) face the observation of this transition is not very clear; it really amounts to a blurring of the intensities around the $p(1 \times 1)$ spots so that the satellites are no longer visible. For the (110) surface a sharp $p(1 \times 1)$ pattern is obtained but only after passing via a $p(1 \times 3)$ structure. The anomalous structures of (110) surfaces have not been fully interpreted (see Rhead 1973); it is interesting to note that a $p(1 \times 3)$ structure is also obtained for cleaned platinum.

The patterns that follow the $p(1 \times 1)$ patterns are interpreted as adsorbed overlayers superimposed on the normal substrate structures. The $p(\sqrt{3} \times \sqrt{3})$ R 30° pattern on (111) can be formally ascribed to the surface mesh shown in figure 2(*a*). This pattern would be produced by adsorption in simple sites: the arrangement is then the one that gives the lead atoms the closest distance of approach compatible with their size. This structure is quickly followed by one that produces the pattern of figure 1(*a*). Here the spots in the outer ring are first order reflexions from the substrate. The inner pairs of extra spots can be ascribed to a compact hexagonal overlayer of lead, rotated with respect to the substrate and with domains in two equiprobable orientations. The model of figure 2(*b*) agrees, within the limits of experimental error, with the observed positions of these extra spots. The ratio of the reciprocal lattice vectors obtained from the pattern agrees with the ratio of the bulk diameters of lead and gold atoms to within 2%. The model actually produces a coincidence lattice with a relatively small mesh. Because of strong modulation by the Fourier transform of the contents of the coincidence mesh one does not observe all the extra spots that might be attributable to this mesh. In fact the only spots observed

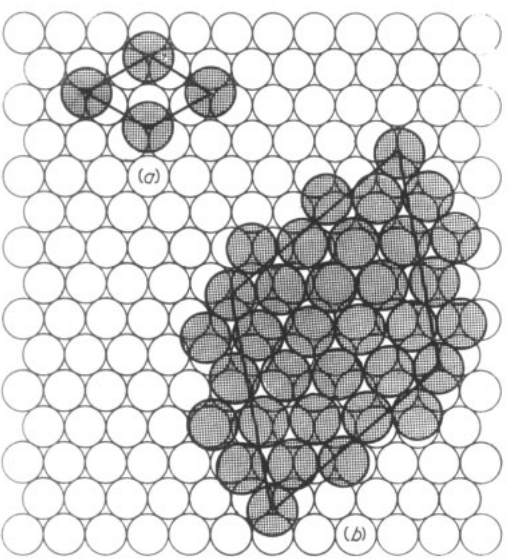

Figure 2. Models of structures on the (111) face. (*a*) A $p(\sqrt{3} \times \sqrt{3})$ R 30° mesh with adsorbed atoms in simple sites. (*b*) A hexagonal overlayer in the orientation that would give spots of one of the domains of figure 1(*a*). In this model the ratio of atomic diameters Pb:Au is 1·21 which coincides with the value for bulk crystals. Patches with dense lead rows parallel to dense gold rows also occur: they give rise to faint spots between the pairs of spots in figure 1(*a*).

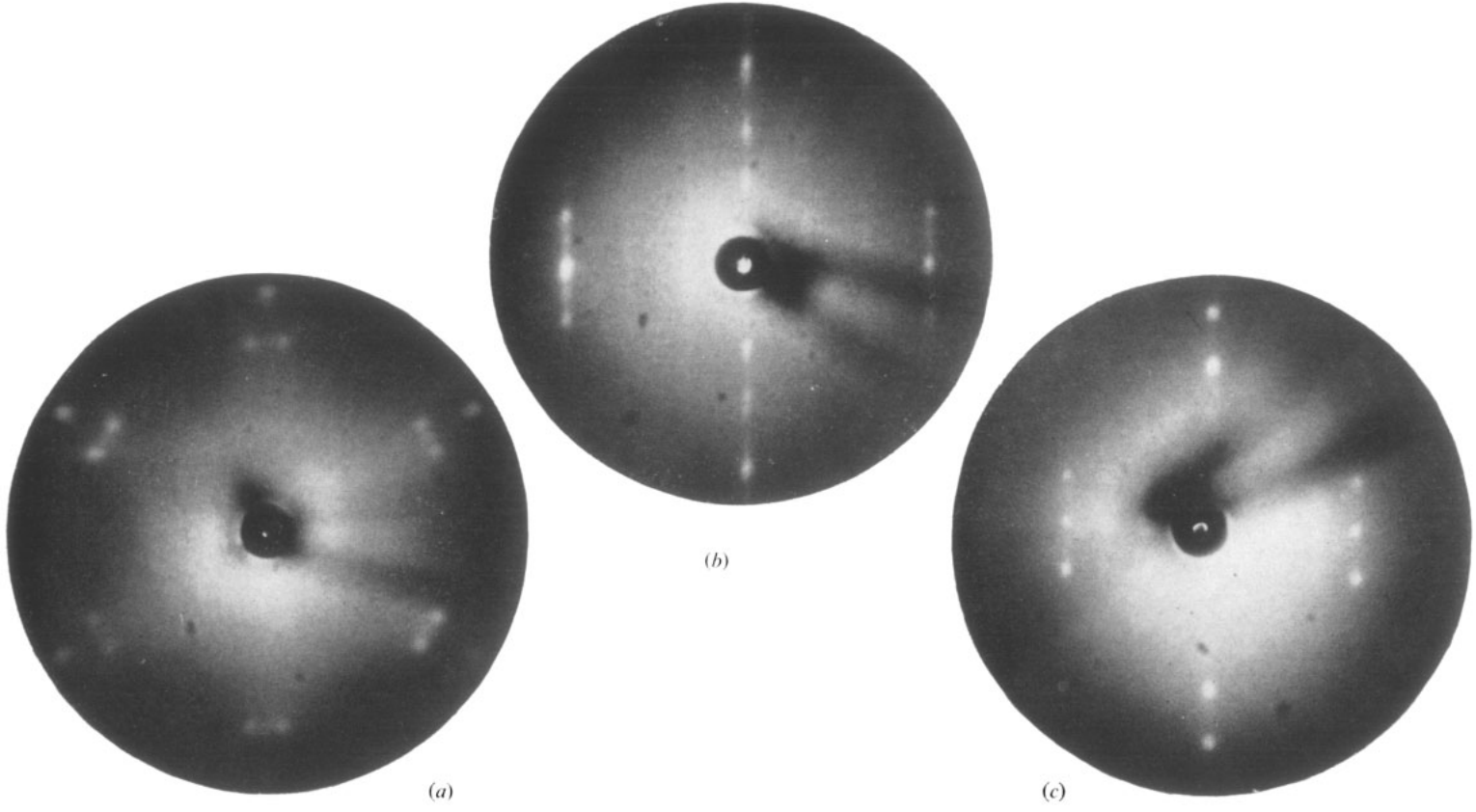

Figure 1. LEED patterns corresponding to complete compact hexagonal monolayers. (*a*) The (111) face; 38 eV. The six spots in the outer ring are first order substrate reflexions. (*b*) The $p(7\times3)$ pattern from the (110) substrate; 40 eV. The threefold periodicity appears as faint streaking. This streaking can be ascribed to irregularities in the coincidence mesh parameter along the atomic grooves while the faintness is due to strong modulation of the intensities by the Fourier transform of the contents of the coincidence mesh. (*c*) The $p(4\times4)$ pattern from the (110) substrate; 47 eV. The second fourfold periodicity appears as a faint streaking similar to that in (*b*).

(facing page 800)

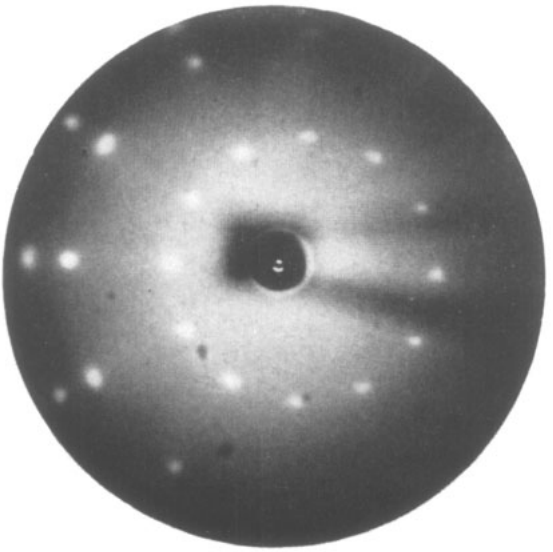

(*a*)

(*b*)

Figure 4. LEED patterns corresponding to surface alloys. (*a*) The (111) surface 545 eV. The crystal has been tilted to reveal more clearly the second order reflexions on one side. (*b*) The (110) face; 195 eV. The pattern shows only the first order reflexions. Alternate spots (spots from domains of one orientation) are slightly streaked.

correspond to the smallest spacing between dense rows of lead. (Delamare and Rhead 1973) give similar examples of strong modulation of coincidence lattice intensities).

At the same time that the pattern of figure 1(*a*) is developing there occur similar compact arrangements on the (100) face—in particular the $c(6 \times 6)$ structure which has also been interpreted as a compact hexagonal overlayer (BR). During this stage the patterns from the (110) face show a 7-fold periodicity in the direction corresponding to the atomic 'groove' on this face. This 7-fold periodicity is easily accounted for by adsorption of dense rows of lead in the atomic grooves of the substrate. This leads first to a $p(7 \times 1)$ structure (figure 3(*a*)) and then, after further deposition, to a $p(7 \times 3)$ pattern

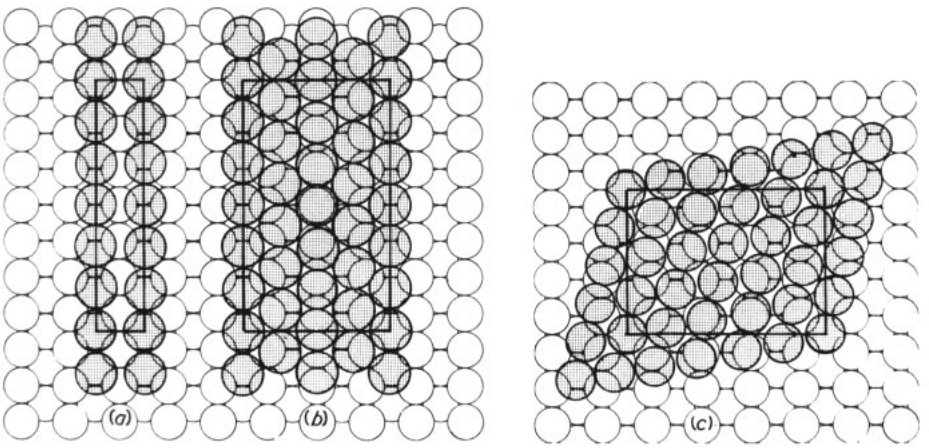

Figure 3. Models of structures on the (110) face. (*a*) The $p(7 \times 1)$ structure. Along the grooves the lead atoms are compressed by about 3·5% compared to their bulk diameter. (*b*) The $p(7 \times 3)$ structure. The projected mean diameter of lead atoms in the dense rows not parallel to substrate grooves coincides with the bulk value. (*c*) Possible interpretation of the $p(4 \times 4)$ pattern. In this structure the average diameter of the lead atoms would be compressed by about 7% compared with the bulk value. The streaking and strong background intensity of figures 1(*b*) and 1(*c*) indicate disorder in the structures 3(*b*) and 3(*c*).

(figure 1(*b*)) which can be interpreted as a compact pseudohexagonal overlayer (figure 3(*b*)). During some of the experiments a $p(4 \times 4)$ pattern was also observed (figure 1(*c*)). This pattern exists only for a short range of coverages. A possible interpretation would be a compact hexagonal overlayer rotated with respect to the $p(7 \times 3)$ structure (figure 3(*c*)). Thus, up to this stage the behaviour of all three faces is very similar. The interpretation of the patterns in terms of the formation of compact hexagonal layers—of approximately the same density on each face—is supported by the AES observations reported in the next section.

From various LEED–AES studies of the first stages of deposition of metallic vapours (see the work cited by BR) it would appear that the observed formation of a compact dense hexagonal, or pseudohexagonal, monolayer is a general result. We would normally expect that the LEED pattern that characterizes the compact monolayer arrangement would mark a final stage in the succession of diffraction patterns: thereafter one would obtain either evidence of multilayer formation, with the disappearance of surface nets in coincidence with the substrate, or evidence of the formation of bulk crystals coexisting with the completed monolayer. In this respect the gold–lead system is quite different

from other systems previously studied in that the monolayer pattern is *rapidly replaced*, on further deposition, by a different final pattern. The final patterns obtained on the (111) and (110) faces are shown in figure 4. These patterns are essentially the same as that observed on the (100) face (BR)—namely, an hexagonal '12 spot' pattern† that can be interpreted as a surface alloy.

The previous interpretation (BR) of the alloy arrangement on the (100) face is incorrect. Inspection of the hexagonal LEED pattern when it coexists with the $c(6 \times 6)$ pattern shows that the mesh parameter is $2a$ and not $4a/\sqrt{3}$ as reported (where a is the atomic diameter of gold). The correct mesh is shown in figure 6. Since this mesh is smaller by 15% than that reported by BR the previously proposed structure with composition $AuPb_3$ is no longer plausible.

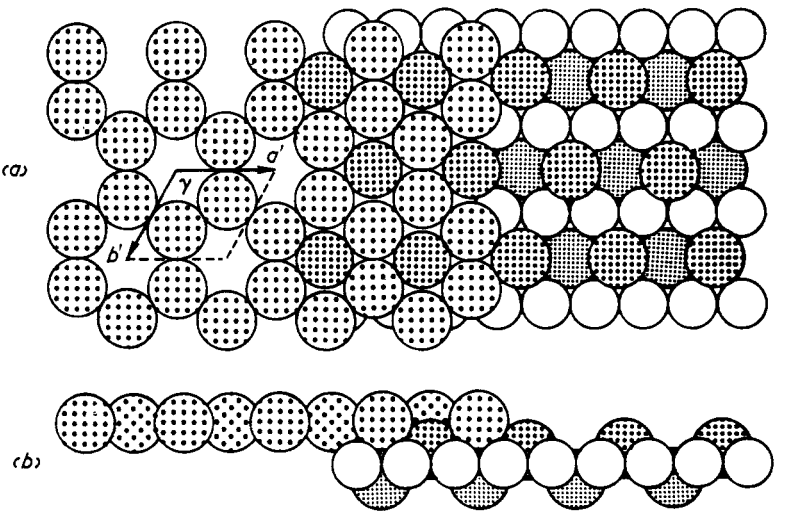

Figure 5. Representation of the structure of $AuPb_2$ parallel to the (110) plane of the bulk crystal. (*a*) top view, (*b*) side view. Lead atoms in grey shaded according to depth. The bulk crystalline structure is bc tetragonal (C16, $CuAl_2$ type) with lattice parameters $a = 7{\cdot}32$ Å, $c = 5{\cdot}65$ Å. The dense rows of gold atoms in the figure are parallel to the c axis of the bulk lattice. The vectors drawn define a *surface* mesh: $a' = c = 5{\cdot}65$ Å, $b' = \{(c/2)^2 + (a/\sqrt{2})^2\}^{1/2} = 5{\cdot}90$ Å, $\gamma = 118{\cdot}6°$. The layers shown, cut away partially to reveal the structure, make up the minimum thickness for one unit of the compound.

There are two main reasons for attributing the 12 spot pattern to a compound arrangement: (i) the relatively large size of the unit mesh is difficult to explain in terms of atoms of one type only, (ii) the results from AES (next section) clearly indicate the presence of both gold and lead in the final arrangement. Without an analysis of the LEED intensities, which we have not attempted, the LEED pattern does not give data relative to the distribution of atoms within the unit mesh. We do not, therefore, have direct access, via LEED, to the composition of the surface compound.

Work on thin films, however, strongly suggests the composition $AuPb_2$. Weaver and Brown (1963) deposited thin film diffusion couples of lead on top of gold and monitored optical reflectivity changes during ageing. The whole of the diffusion data thus obtained pointed to the formation of $AuPb_2$ and the presence of this compound was confirmed by

† Concentric rings, each of twelve spots, produced by two orthogonal hexagonal nets.

electron diffraction analysis. Chauvineau and Pariset (1974) have measured electrical resistivity changes in thin gold films at ambient temperature during deposition of monolayer quantities of lead. The amount deposited was controlled by a quartz crystal oscillator. After completion of the first monolayer there was observed the start of a sharp increase in resistivity due to thinning of the gold film and formation of a compound. An x ray diffraction analysis of thick layers of this compound identified it as $AuPb_2$. In the light of the above results the most plausible interpretation of the 12 spot LEED patterns appears to be based on the compound structure shown in figure 5 which is a succession of dense layers of the bulk crystalline structure of $AuPb_2$ parallel to the bulk (110) plane.

The surface mesh of figure 5 is pseudohexagonal with about 4% difference in the unit vectors. Measurements of the 12 spot patterns from the (100) and (111) substrates show that the observed surface mesh is actually much closer to hexagonal ($a' = b' \pm 1{\cdot}5\%$ and $\gamma = 120° \pm 1{\cdot}5°$). It is possible that epitaxy with the substrate modifies slightly the parameters of the compound structure. For example, the c-vector of the bulk compound, 5·65 Å, could be expanded by about 2% to make it fit the distance between simple sites (figure 6). Such a deformation would make the mesh of figure 5 close to hexagonal.

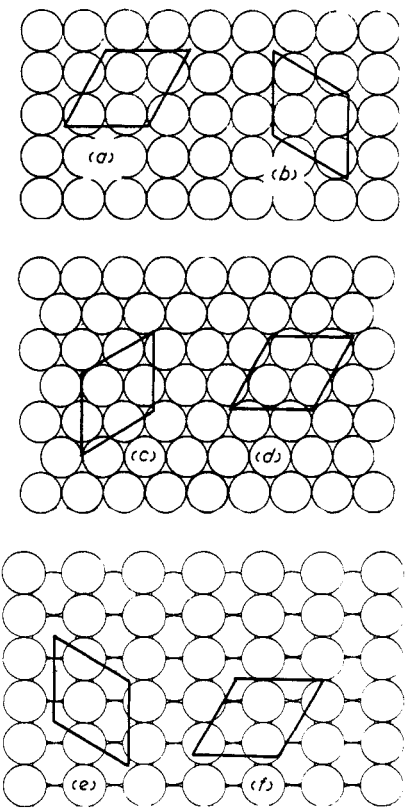

Figure 6. Representation of the observed meshes of the alloy structure related to simple sites on the different substrates. (*a*) and (*b*) are equivalent. The unit vector of (*c*) is 1% larger than that of (*d*); the arrangement corresponding to (*c*) appears first during deposition. The streaking of some of the spots in figure 4(*b*) indicates that domains corresponding to (*f*) take up a small range of orientations with small rotations about the surface normal.

Deformations probably occur also in the top layers of the substrate as well as in the compound layer.

The relationship between the observed meshes corresponding to the 12 spot patterns and the different substrate meshes is shown in figure 6. For the (100) substrate the two orthogonal orientations are strictly equivalent. This is obviously not the case for the other substrates and as a result certain differences appear in the LEED patterns (see captions to figures 4 and 6).

For all three substrates the alloy pattern rapidly replaces the compact monolayer pattern and at no stage does the alloy pattern give rise to an observable coincidence mesh linking it either to the substrate or to the first monolayer. BR stated that this evidence suggests that the alloy arrangement is initiated in the second layer and that when this occurs the first monolayer is also transformed to the alloy structure: the alloy always has a minimum thickness greater than a monolayer. It is clear from figure 5 that the smallest unit of the alloy structure must necessarily involve more than one layer of lead.

3. Results from Auger spectroscopy

Typical results from AES are shown in figure 7. These data were obtained under identical conditions for both faces (but at a slightly lower deposition rate than that corresponding to table 1). Comparison with the earlier results of BR shows that the plots for the Auger signals from each of the three faces exhibit the following common features: for the lead signal there is (i) an initially linear rise up to the time needed for the full development of the LEED pattern that corresponds to a compact monolayer, (ii) a sharp knee that always

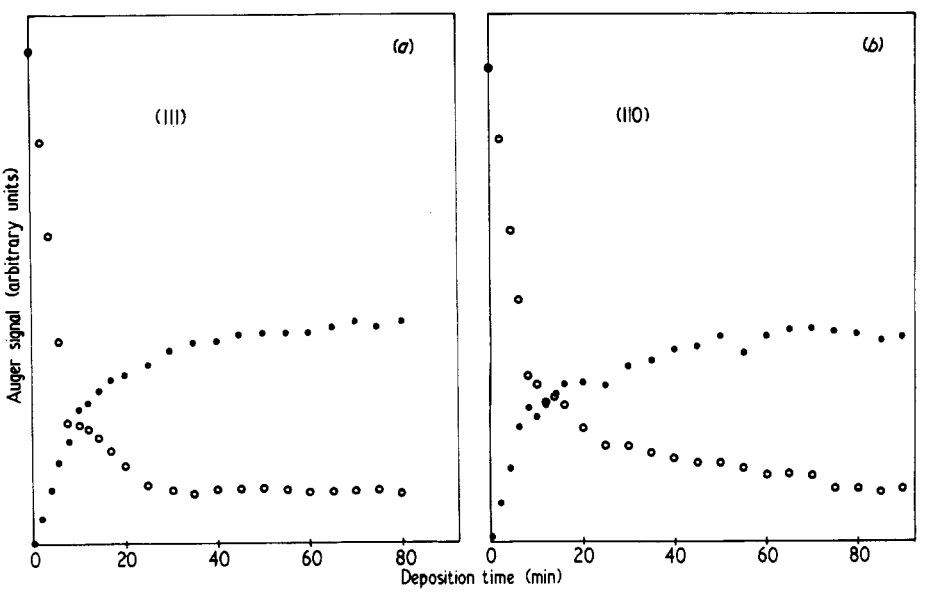

Figure 7. Peak to peak signals of the differentiated Auger spectrum for Au (71 eV) (○) and Pb (93 eV) (●) as a function of deposition time during a typical run. (*a*) the (111) face, (*b*) the (110) face. The patterns for the completed first monolayer are observed in the region of the first knee in the lead signal.

precedes the observation of the LEED pattern attributed to the alloy arrangement, (iii) a slow rise up to a final plateau value. For the gold signal there occurs (iv) an initial rapid decrease, (v) a change in slope at the same time as the knee in the plot for the lead signal, (vi) a further decrease towards a final nonzero plateau value.

These features have been discussed, in terms of the (100) face, by BR. It appears that the conclusions can be generalized to all three low index faces. The first sharp knees in the plots for the lead and gold signals correspond to the completion of the compact lead monolayer. This interpretation is supported by theoretical models for AES of deposited films (Gallon 1969, Seah 1972) and by experimental observations on other systems (Jackson *et al* 1973, Bauer 1973). It is also confirmed by the LEED observations. The remaining parts of the curves correspond to a layer-by-layer growth of the alloy arrangement: formation of an alloy explains, in particular, the nonzero plateau value of the gold signal. The continued rise of the lead signal clearly indicates layer growth (it is known from the work cited above that a plateau value is reached for thick films) but if the thickening film were pure lead the gold signal would decay to zero. The argument against an alternative explanation of the nonzero gold signal—an agglomeration of the lead deposit—has been given by BR.

For the same experimental run the main features of the Auger data are quantitatively the same for all three faces. Within experimental error the first knees occur at the same point: the initial sticking probability and the density of the compact monolayer show no significant differences. Slight differences occur in the form of the plots between the first monolayer and the final plateau values. Thus, for the (110) face the gold signal appears to descend more slowly towards the plateau. One feature that was frequently, but not always, observed is a small kink in the plot of the lead signal in the region of the first knee (see figure 7(*b*)).

4. Conclusions

The combination of LEED and AES has proved to be a powerful means for studying the deposition of one metal on another. In comparison with previous systems that have been studied, the deposition of lead on gold exhibits important differences that can be clearly ascribed to spontaneous formation of a surface alloy. The results obtained for the (100), (111) and (110) substrate faces, and particularly the observation of the same final LEED pattern from all three faces, constitute a body of evidence for the appearance of the alloy. Several features of this system, notably the possibility of observing the phenomenon at ambient temperature and the ease of maintaining the substrate surfaces clean in the vacuum chamber, suggest its suitability for studies by other techniques of surface spectroscopy.

Acknowledgments

This work has been carried out with the support of the Centre National de la Recherche Scientifique and the Délégation Générale à la Recherche Scientifique et Technique (contract No 71-72782).

We thank M M Chauvineau and Pariset for communicating their work and Professeur J Bénard for his encouragement.

References

Bauer E G 1973 *Colloque de physique et de chimie des surfaces, SFITV, Brest*
Biberian J P and Rhead G E 1973 *J. Phys.* F: *Metal Phys.* **3** 675–82
Chauvineau J P and Pariset C 1974 to be published
Delamare F and Rhead G E 1973 *Surface Sci.* **35** 172–84, 185–93
Gallon T E 1969 *Surface Sci.* **17** 486–9
Grønlund F and Nielsen P E H 1972 *J. appl. Phys.* **43** 3919–21
Jackson D C, Gallon T E and Chambers A 1973 *Surface Sci.* **36** 381–94
Palmberg P W and Rhodin T N 1967 *Phys. Rev.* **161** 586–8
—— 1968 *J. chem. Phys.* **49** 134–46, 147–55
Rhead G E 1973 *J. Phys.* F: *Metal Phys.* L53–6
Seah M P 1972 *Surface Sci.* **32** 703–28
Weaver C and Brown L C 1963 *Phil. Mag.* **8** 1379–93
Wood E A 1964 *J. appl. Phys.* **35** 1306–12